Letter

Hubbard model on a triangular lattice: The role of charge fluctuations

Ji-Si Xu,[1] Zheng Zhu,[2,3,*] Kai Wu,[4] and Zheng-Yu Weng[1,†]

[1]*Institute for Advanced Study, Tsinghua University, Beijing 100084, China*

[2]*Kavli Institute for Theoretical Sciences, University of Chinese Academy of Sciences, Beijing 100190, China*

[3]*CAS Center for Excellence in Topological Quantum Computation, University of Chinese Academy of Sciences, Beijing 100190, China*

[4]*Manifold Creative Global, 100 Lorong 23 Geylang, 388398, Singapore*

(Received 17 October 2023; revised 25 January 2024; accepted 7 February 2024; published 27 February 2024)

A chiral spin liquid (CSL) phase has been recently reported in the Hubbard model on a triangular lattice. It emerges in an intermediate coupling regime at half-filling, which is sandwiched between a 120° antiferromagnetic (AFM) phase and a metallic phase as a function of on-site repulsion U. In this work, we examine the mechanism of the CSL and complex phase diagram via analytic analysis and numerical density matrix renormalization group (DMRG) method. First, we identify an exact Berry-phase-like sign structure in the partition function of the model at arbitrary U, which is originated from the Fermi sign structure at $U = 0$.The spin and charge degrees of freedom are generally entangled via a singular phase string in such a many-body sign structure. In the large-U limit, the suppression of the charge fluctuation at half-filling can render the phase string ineffective, resulting in the AFM order. However, if one precisely switches off such a phase string in the DMRG calculation, the 120° AFM is shown to survive all the way down to a much weaker U without the emergence of the CSL and metallic phases. It indicates that the phase-string sign structure plays the key role to mediate the mutual interaction between the charge and spin fluctuations, which results in the CSL and metallic phases at finite U. General implications for the Mott physics in the Hubbard model will also be discussed.

DOI: 10.1103/PhysRevB.109.L081116

Introduction. The quantum spin liquid (QSL) has been a subject with growing interest since the concept was first introduced by Anderson in the 1970s [1–6]. The antiferromagnetic (AFM) spin system on triangular lattice was once believed to be a promising candidate to realize a QSL state due to its strong geometric frustration. But the numerical studies have revealed that in the Heisenberg model, the ground state is actually 120° AFM long-range ordered [7,8]. Experimentally some triangular lattice materials like $Ba_3CoSb_2O_9$ [9–14] clearly exhibit a 120° AFM order. On the other hand, several candidate materials with triangular lattice, such as the organic Mott insulators κ-(BEDT-TTF)$_2$Cu$_2$(CN)$_3$ [15–18] and EtMe$_3$Sb[Pd(dmit)$_2$]$_2$ [19–21], have been considered potentially as the QSL systems.

In contrast to the Heisenberg model with spin local moment, a QSL phase in a Hubbard model at half-filling with an intermediate strength of U has been recently reported [22–28]. Such a QSL phase is located between the metallic regime at small U and the 120° AFM phase at large-U, where the latter is continuously connected to the Heisenberg model in the large-U limit. In particular, this QSL has been further identified as a chiral spin liquid (CSL) [26,27].

Whereas the geometric frustration alone in the Heisenberg model on a triangular lattice is not enough to drive the system into a quantum disordered phase, the QSL discovered in the Hubbard model may be attributed to the fact that an increasing charge fluctuation with reducing U plays an important role. Among the numerous theories for QSL, the interplay between the spin and the charge degrees of freedom has been discussed [29–33]. But most theories have assumed *a priori* the existence of QSL with the focus on the Mott transition to a metallic phase.The charge fluctuation may lead to a high-order spin interaction [34] to stabilize the QSL state. The numerical results [35] show that a Heisenberg model with four spin term or other additional terms can give rise to a rich phase diagram, including the QSL phase.Nevertheless, how the charge fluctuations systematically influence the spin order and *vice versa* with reducing U/t, including the Mott transition, still remains elusive as the central challenge in strongly correlated systems.

In this paper, we investigate the mechanism of how the charge fluctuation frustrates the 120° AFM order as U reducing from the strong-coupling limit. We first analytically identify the precise sign structure of the triangular lattice Hubbard model at an arbitrary U, temperature, and doping concentration based on the partition function. It is shown that the charge and spin degrees of freedom are intrinsically entangled via a novel sign structure known as the phase string, besides the conventional fermions statistics associated with the charge (holons and doublons) and some geometric Berry phase associated with the triangular lattice. The same kind of phase-string factor has been previously identified on the square lattice for the Hubbard model without the additional frustration of the geometric phase [36]. Its large-U version has also been previously found in the t-J model for both square lattice [37,38] and triangular lattice [39].

*zhuzheng@ucas.ac.cn

†weng@mail.tsinghua.edu.cn

Then by "switching off" the phase-string (without changing the other phase factors and path-dependent weight) in a density matrix renormalization group (DMRG) calculation, we show that the CSL and metallic phases disappear in the phase diagram, with only the AFM state persisting all the way down to a much weaker U at half-filling. It clearly indicates that the charge fluctuations must be mediated by the phase-string sign structure in order to twist the AFM into a QSL in the intermediate U/t. Namely, without the phase string, the charge and spin correlations become effectively decoupled. In general, it implies that the Mott physics is dictated by the novel sign structure hidden in the Hubbard model, which should be treated explicitly and carefully in order to properly understand the interplay between the spin and charge dynamics including the opening/closing of the charge (Mott) gap.

Sign Structure of the Hubbard Model.— In this work, we shall study the Hubbard model,

$$H_{\rm Hub} = H_t + U\sum_i n_{i\uparrow}n_{i\downarrow}, \tag{1}$$

where $H_t \equiv -t\sum_{\langle ij\rangle,\sigma} c^\dagger_{i\sigma}c_{j\sigma} + H.c.$ denotes the nearest neighbor (NN) hopping on a triangular lattice.

We shall first identify an exact sign structure in the partition function as follows:

$$Z_{\rm Hub} \equiv {\rm tr}(e^{-\beta H_{\rm Hub}}) = \sum_c S[c]W[c], \tag{2}$$

where $W[c] \geqslant 0$ is a positive weight, while $S[c]$ with $|S[c]| = 1$ denotes the sign structure for any closed loop c of the spin and charge coordinates in the full Hilbert space. The proof is based on the high-temperature ($T = 1/\beta$) series expansion of the partition function to all orders:

$$Z_{\rm Hub} = \sum_{n=0}^{\infty}\frac{\beta^n}{n!}\sum_{\{\alpha_i\}_{i=1}^n}\prod_i \langle\alpha_{i+1}|(-H_{\rm Hub})|\alpha_i\rangle, \tag{3}$$

where α is the label of a complete set of basis composed of the spin(on) (in the S^z quantization) and chargon coordinates at single occupied and empty/double occupied sites (see the Supplemental Material in Ref. [40]). We can view $c = \{\alpha_i\}_{i=1}^n$ as a closed loop in the coordinate space with $|\alpha_1\rangle = |\alpha_{n+1}\rangle$.

Here $S[c]$ collects all the signs of the matrix elements $\langle\alpha_{i+1}|(-H_{\rm Hub})|\alpha_i\rangle$ to give rise to [40]

$$S[c] \equiv S_0[c]\times(-1)^{N^{\rm ch}_{\rm ex}[c]}\times\tau_{\rm ph}[c], \tag{4}$$

where

$$S_0[c] \equiv (-1)^{N^{\uparrow}[c]}. \tag{5}$$

Here $N^{\uparrow}[c]$ denotes the total steps of hopping of $\uparrow$ spinons in a closed loop c; $(-1)^{N^{\rm ch}_{\rm ex}[c]}$ counts the fermion signs pending on $N^{\rm ch}_{\rm ex}[c]$ as the total exchange number between the holons and between the doublons as the identical particles. The third factor in Eq. (4) is the most exotic which indicates a *mutual statistics* between the chargons and spinons

$$\tau_{\rm ph}[c] \equiv (-1)^{N^h_{\downarrow}[c]}\times(-1)^{N^d_{\uparrow}[c]}, \tag{6}$$

in which $N^h_{\downarrow}[c]$ and $N^d_{\uparrow}[c]$ count the total number of swaps between the chargons and spinons, i.e., a holon and a $\downarrow$-spinon, and a doublon and an $\uparrow$-spinon, respectively, in the closed loop c. The basic processes within a closed loop c and the associated sign structure are figuratively illustrated in Fig. 1.

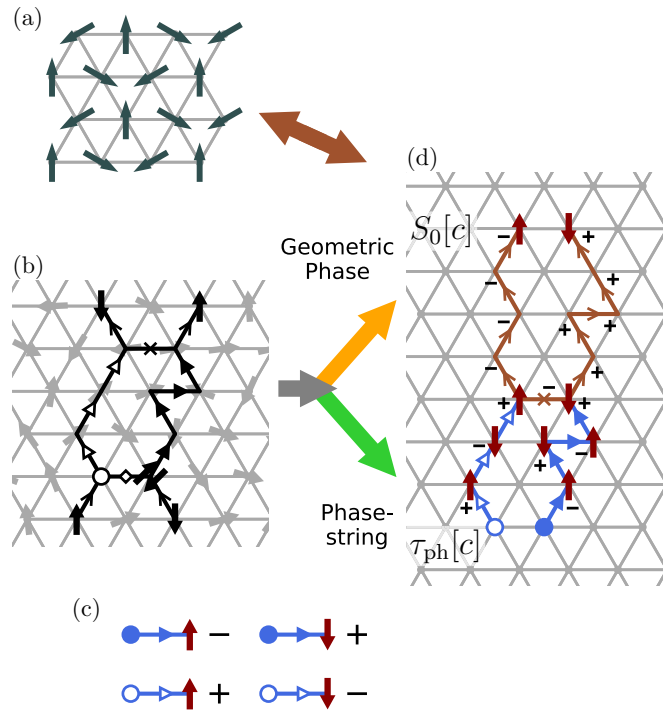

FIG. 1. The illustration of the sign structure of the triangular Hubbard model as given in Eq. (4). (a) A typical spin configuration of 120° AFM order at large-U; (b) Charge fluctuations as spontaneous creation (at link marked by an open diamond) and annihilation (at link marked by the cross) of the holon (open circle) and doublon at half-filling; (c) Elementary processes of the hopping of the chargon (doublon, filled circle and holon, open circle) and the associated signs, $\pm$, depending on the spin swapped with the chargon. They contribute to the phase string $\tau_{\rm ph}$ in Eq. (6) for the chargon hoppings as illustrated in (d); Each up-spin hopping on the lattice will acquire an additional geometric $(-)$ sign [cf. (d)], which gives rise to a geometric phase S_0 in Eq. (5); Finally, it is noted that the chargons will contribute to an additional minus sign in Eq. (4) each time two identical holons or doublons are exchanged as if they are fermions (not shown here in the figure).

It is noted that previously a similar sign structure has been exactly identified [36] for the two-dimensional (2D) Hubbard model on a square lattice, in which $S_0[c] = 1$ in Eq. (4) without the geometric frustration. Here for the triangular lattice, $S_0[c]$ is nontrivial which depends on the parity of the total triangular units enclosed within the closed paths of the $\uparrow$-spinons. In the large-U, i.e., the Heisenberg limit at half-filling, it will be responsible for driving the system into the 120° AFM order (see below). The fermion statistical sign factor associated with the chargons is also conventional, which is similar to doping a semiconductor. Inside the sign structure in Eq. (4), the sign factor $\tau_{\rm ph}[c]$ introduces a novel long-range mutual entanglement between the spin and charge degrees of freedom, which is known as the phase-string whose nontrivial effect has been previously studied in the doped cases on a square lattice in the large-U limit [41,42].

To examine its unique effect, one may exactly switch off $\tau_{\rm ph}[c]$ in Eq. (4), with the partition function reducing to

$$Z_{\sigma\text{-Hub}} \equiv \mathrm{tr}(e^{-\beta H_{\sigma\text{-Hub}}}) \equiv \sum_c S_0[c](-1)^{N_{\rm ex}^{\rm ch}[c]} W[c] \quad (7)$$

with the same weight $W[c]$ [40]. It is straightforward to show that the corresponding Hamiltonian is modified as [40] $H_{\sigma\text{-Hub}} = H_{\sigma t} + U\sum_i n_{i\uparrow}n_{i\downarrow}$ where

$$H_{\sigma t} \equiv -t\sum_{\langle ij\rangle,\sigma} c^\dagger_{i\sigma}c_{j\sigma}\left[\sigma\hat{P}^T_{ij} + \left(1-\hat{P}^T_{ij}\right)\right] + \mathrm{H.c.} \quad (8)$$

with $\hat{P}^T_{ij}$ a projection operator to enforce a single chargon (holon or doublon) at the NN bond ij, whose hopping involves an exchanging with a spinon [cf. Fig. 1(c)]. By contrast, the projection $(1-\hat{P}^T_{ij})$ involves a simultaneous creation or annihilation of a pair of holon-doublon at ij.

Therefore, the sole distinction between the Hubbard and σ-Hubbard models lies in the presence and absence of the phase-string factor of Eq. (6) in their respective sign structures [cf. Eqs. (2) and (7)]. Physically the phase-string of Eq. (6) will dynamically entangle the charge and spin degrees of freedom in the Hubbard model, which otherwise may behave independently of each other in a more conventional manner in the σ-Hubbard model (see below).

Phase diagram at half-filling: DMRG results. To precisely characterize the distinction between the Hubbard model and σ-Hubbard models, we employ the DMRG algorithm to examine the ground state properties *at half-filling* in the remainder of the paper. The triangular lattice is spanned by the primitive vectors $\mathbf{e_x} = (1, 0)$, $\mathbf{e_y} = (1/2, \sqrt{3}/2)$ and wrapped on cylinders with circumference of 4 along the y direction (cf. Fig. S1 in Ref. [40]). Depending on the nature of distinct phases, the bond dimension $\mathcal{D}$ is pushed up to $\mathcal{D} = 24000$ to secure the convergence.

In Fig. 2, the characteristics of the spin degrees of freedom are shown in the intermediate U/t regime. Figures 2(a) and 2(b), present the results for the Hubbard model, in which three typical phases are shown. To identify the 120° AFM order, we compute the spin structure factor $S(\mathbf{q})$, which is defined as $S(\mathbf{q}) = 1/N\sum_{ij}\langle \mathbf{S}_i\cdot\mathbf{S}_j\rangle e^{i\mathbf{q}\cdot(\mathbf{r}_i-\mathbf{r}_j)}$. As shown in Fig. 2(a), $S(\mathbf{q})$ is peaked at $\mathbf{q} = \mathbf{K}^*$, characterizing the 120° AFM order at large-U side, where $\mathbf{K}^*$ is the closest allowed momentum to $\mathbf{K}$ as the characteristic momentum of the 120° AFM order. Then a CSL order as characterized by the order parameter $|\langle \mathbf{S}_i\cdot(\mathbf{S}_j\times\mathbf{S}_k)\rangle|$ sets in over an intermediate regime approximately between $8.5 < U/t < 10.7$ [see Fig. 2(b)], where the peaked spin structure factor $S(\mathbf{K}^*)$ gets diminished. As U/t continues to decrease further, the CSL order eventually vanishes and the system enters a metallic phase at $U/t \approx 8.5$. Such an insulator-to-metal transition can also be identified by the close of the charge gap $\Delta_c = \frac{1}{2}[E_0(N_\uparrow+1, N_\downarrow+1) + E_0(N_\uparrow-1, N_\downarrow-1) - 2E_0(N_\uparrow, N_\downarrow)]$, as shown in Fig. 3(a), here $E_0(N_\uparrow, N_\downarrow)$ denotes the ground-state energy of a system with $N_\uparrow$ spin-up electrons and $N_\downarrow$ spin-down electrons, and $N_\uparrow = N_\downarrow = N/2$ at half filling. We remark that these results are consistent with the previous study [26].

By contrast, the corresponding DMRG results for the σ-Hubbard model are also presented in Figs. 2(d) and 2(c) for the spin part and in Fig. 3 for the charge part, respectively. As

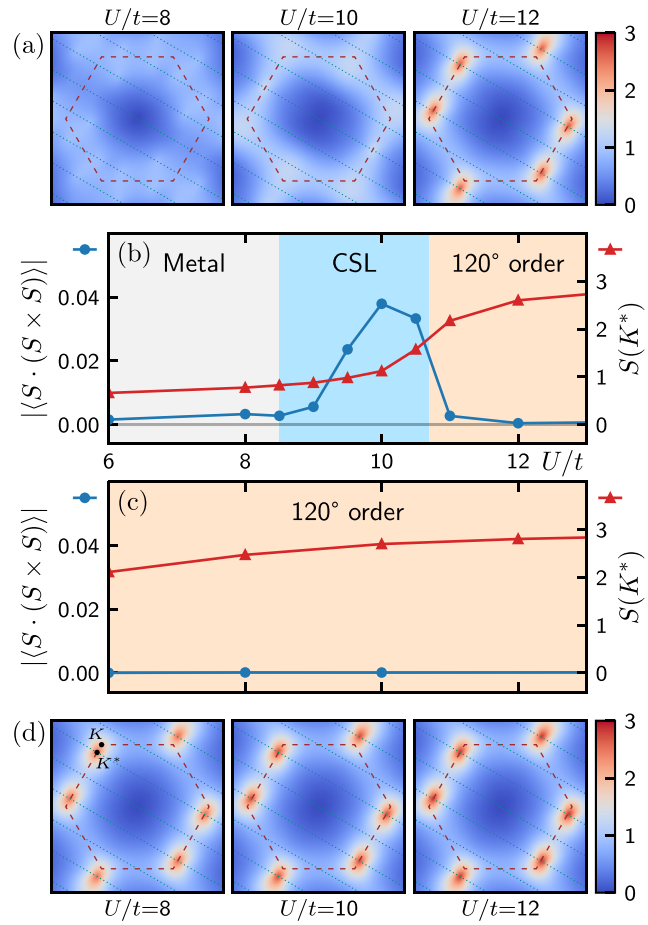

FIG. 2. The spin characterizations of the phase diagram in the triangular Hubbard model and σ-Hubbard model by DMRG calculation. (a) and (d): The momentum distributions of the spin structure factor $S(\mathbf{q})$ at $U/t = 8$, 10, 18, respectively. The three distinct phases of the Hubbard model in (a) reduce to a single phase in the σ-Hubbard model [(d)]; (b) and (c): The chiral order parameter $|\langle \mathbf{S}_i\cdot(\mathbf{S}_j\times\mathbf{S}_k)\rangle|$ (blue) and the spin structure factor at K^* (red), for the Hubbard model [(b)] and the σ-Hubbard model [(c)], respectively.

one can see, the phase diagram is totally changed from that of the Hubbard model: in the whole parameter regime of U/t that we inspect, the 120° AFM order always remains dominant as the sole stable phase with no more CSL phase. Here the charge gap remains finite [cf. Fig. 3(a)] and is persistent down to $U/t \approx 2$. Furthermore, in Fig. 3(b) the double-occupancy per site, D/N, exhibits a fast increase in the CSL region of the Hubbard model from the larger U. For the σ-Hubbard model, however, D/N evolves much more smoothly and flatly over the whole region, and so does the corresponding single-electron momentum distribution n_k in Fig. 3(d), in contrast to a sharper Fermi-sea-like feature in the metallic phase of the Hubbard model at $U/t = 8.5$ [cf. Fig. 3(c)]. In general, the charge fluctuations are found to be well decoupled from the 120° AFM spin order in the σ-Hubbard model, in which one does not encounter a phase transition with U/t reducing from the strong coupling to the order of one, in sharp contrast to the three phases identified in the Hubbard case at $U/t > 8$.

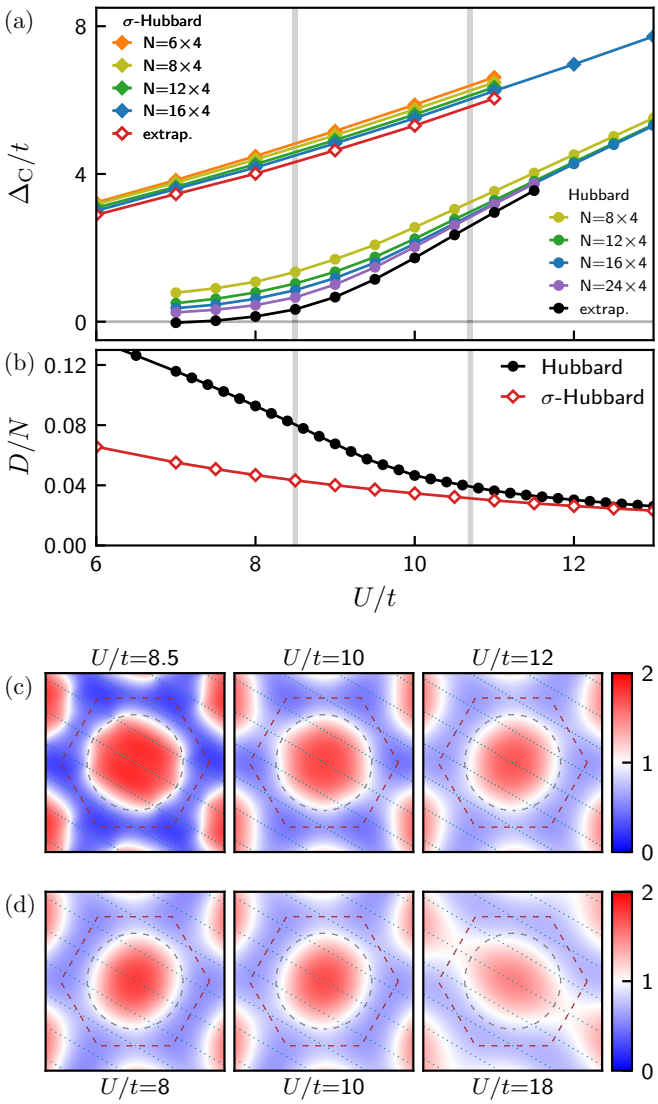

FIG. 3. The charge characterizations of the Hubbard and σ-Hubbard models. (a) The charge gap; (b) The average double occupancy. The vertical lines: two phase transition points of the Hubbard model; (c) and (d) Electron momentum distribution n_k for the Hubbard and σ-Hubbard models, respectively.

Discussion. There is no essential distinction between the Hubbard and σ-Hubbard models in the large U/t limit, where the spins are governed by the Heisenberg model while the charge sector is well gapped. Note that the two models only differ by the phase string in the partition function. The sharp distinction between the two models with reducing U should be thus entirely attributed to the phase string that mediates the mutual coupling between the spin and charge degrees of freedom. In other words, the emergence of the CSL as well as the Mott transition to a metallic phase in the Hubbard model, which is absent in the σ-Hubbard model, has to be understood by the phase-string effect in the former.

For example, in the large-U limit with the chargon excitations monotonically suppressed at half-filling, the residual sign structure still functioning in Eq. (4) is essentially the conventional Berry phase left [Eq. (5)], whose geometric frustration due to triangular lattice leads to the 120° AFM order of the spins. At $\sim 8.5 < U/t < 10.7$, with reducing the charge gap and increasing D/N, the charge fluctuation must influence the spin part via the phase string such that the AFM order is driven into the CSL phase in the Hubbard model but remains unchanged in the σ-Hubbard model. Note that the charge fluctuation is also self-consistently enhanced within the gapped CSL spin phase in the former. Eventually a metallic phase at smaller $U/t \lesssim 8.5$ with the Mott gap closing up, should be also due to the phase-string, since in the σ-Hubbard model the charge and spin fluctuations remain decoupled similar to the large-U/t case with the 120° AFM order persisting all the way down to a much smaller U/t without encountering the CSL or metallic phase transition.

It is important to realize that for both the Hubbard and σ-Hubbard models, the amplitude $W[c]$ for each path c in the partition functions remains the same. It depends on the amplitudes of t, U, and temperature, and is expected to be a smooth functional of the path c, which is in sharp contrast to the phase-string sign structure [Eq. (6)]. The latter is singular as its sign changes with merely a spin-flip in the total spins exchanging with a chargon for any path c. As the sole distinction between the two models, the phase-string strongly influences both the spin and charge sectors of the Hubbard model by a quantum interference effect under the summation of all the closed paths in an intermediately strong U. Similar to the square lattice case [36,38], by a duality transformation, one may exactly map the phase-string effect into a topological (mutual Chern-Simons) gauge structure [36,41,42] in which the fractionalized spin and charge degrees of freedom are mutually coupled, and this framework has been previously generalized to the triangular lattice t-J model at large doping [39]. It will be very interesting to see how the CSL and the metallic phase as revealed by DMRG may naturally arise from such a gauge interaction, which will be explored elsewhere by a perturbative approach.

Furthermore, the sign structure identified here for the triangular Hubbard model is exact at arbitrary U, doping, and temperature, as well as sample size and dimensionality. Therefore, a systematic exploration based on the Hubbard and σ-Hubbard models using the finite-size exact numerical methods may be also very useful to understand such strongly correlated systems at finite doping [43–51]. Recently a contrasted DMRG study based on the sign structure has provided new insights into the origin of superconducting and charge-density-wave orders at finite doping in the t-t'-J model on square lattice [52]. A similar approach for the triangular lattice may also be interesting in the large-U limit at finite doping [53–58], where the phase-string effect associated with the doped holes/electrons in Eq. (4) becomes singularly important.

Acknowledgments. We acknowledge stimulating discussions with J.-X. Zhang. J.-S.X. and Z.-Y.W. were supported by MOST of China (Grant No. 2021YFA1402101) and NSF of China (Grant No. 12347107); Z.Z. was supported by the National Natural Science Foundation of China (Grant No. 12074375), Innovation Program for Quantum Science and Technology (Grant No. 2-6), the Strategic Priority Research Program of CAS (Grant No. XDB33000000) and the Fundamental Research Funds for the Central Universities.

[1] P. W. Anderson, Resonating valence bonds: A new kind of insulator? Mater. Res. Bull. **8**, 153 (1973).

[2] L. Balents, Spin liquids in frustrated magnets, Nature (London) **464**, 199 (2010).

[3] L. Savary and L. Balents, Quantum spin liquids: A review, Rep. Prog. Phys. **80**, 016502 (2017).

[4] Y. Zhou, K. Kanoda, and T.-K. Ng, Quantum spin liquid states, Rev. Mod. Phys. **89**, 025003 (2017).

[5] J. Knolle and R. Moessner, A field guide to spin liquids, Annu. Rev. Condens. Matter Phys. **10**, 451 (2019).

[6] C. Broholm, R. J. Cava, S. A. Kivelson, D. G. Nocera, M. R. Norman, and T. Senthil, Quantum spin liquids, Science **367**, eaay0668 (2020).

[7] L. Capriotti, A. E. Trumper, and S. Sorella, Long-range Néel order in the triangular Heisenberg model, Phys. Rev. Lett. **82**, 3899 (1999).

[8] S. R. White and A. L. Chernyshev, Neél order in square and triangular lattice Heisenberg models, Phys. Rev. Lett. **99**, 127004 (2007).

[9] Y. Shirata, H. Tanaka, A. Matsuo, and K. Kindo, Experimental realization of a spin-1/2 triangular-lattice Heisenberg antiferromagnet, Phys. Rev. Lett. **108**, 057205 (2012).

[10] T. Susuki, N. Kurita, T. Tanaka, H. Nojiri, A. Matsuo, K. Kindo, and H. Tanaka, Magnetization process and collective excitations in the $S = 1/2$ triangular-lattice Heisenberg antiferromagnet $Ba_3CoSb_2O_9$, Phys. Rev. Lett. **110**, 267201 (2013).

[11] G. Koutroulakis, T. Zhou, Y. Kamiya, J. D. Thompson, H. D. Zhou, C. D. Batista, and S. E. Brown, Quantum phase diagram of the $S = \frac{1}{2}$ triangular-lattice antiferromagnet $Ba_3CoSb_2O_9$, Phys. Rev. B **91**, 024410 (2015).

[12] G. Quirion, M. Lapointe-Major, M. Poirier, J. A. Quilliam, Z. L. Dun, and H. D. Zhou, Magnetic phase diagram of $Ba_3CoSb_2O_9$ as determined by ultrasound velocity measurements, Phys. Rev. B **92**, 014414 (2015).

[13] J. Ma, Y. Kamiya, T. Hong, H. B. Cao, G. Ehlers, W. Tian, C. D. Batista, Z. L. Dun, H. D. Zhou, and M. Matsuda, Static and dynamical properties of the spin-1/2 equilateral triangular-lattice antiferromagnet $Ba_3CoSb_2O_9$, Phys. Rev. Lett. **116**, 087201 (2016).

[14] S. Ito, N. Kurita, H. Tanaka, S. Ohira-Kawamura, K. Nakajima, S. Itoh, K. Kuwahara, and K. Kakurai, Structure of the magnetic excitations in the spin-1/2 triangular-lattice Heisenberg antiferromagnet $Ba_3CoSb_2O_9$, Nat. Commun. **8**, 235 (2017).

[15] Y. Shimizu, K. Miyagawa, K. Kanoda, M. Maesato, and G. Saito, Spin liquid state in an organic Mott insulator with a triangular lattice, Phys. Rev. Lett. **91**, 107001 (2003).

[16] Y. Kurosaki, Y. Shimizu, K. Miyagawa, K. Kanoda, and G. Saito, Mott transition from a spin liquid to a Fermi liquid in the spin-frustrated organic conductor $\kappa-(ET)_2Cu_2(CN)_3$, Phys. Rev. Lett. **95**, 177001 (2005).

[17] S. Yamashita, Y. Nakazawa, M. Oguni, Y. Oshima, H. Nojiri, Y. Shimizu, K. Miyagawa, and K. Kanoda, Thermodynamic properties of a spin-1/2 spin-liquid state in a κ-type organic salt, Nat. Phys. **4**, 459 (2008).

[18] M. Yamashita, N. Nakata, Y. Kasahara, T. Sasaki, N. Yoneyama, N. Kobayashi, S. Fujimoto, T. Shibauchi, and Y. Matsuda, Thermal-transport measurements in a quantum spin-liquid state of the frustrated triangular magnet κ-(BEDT-TTF)$_2$Cu$_2$(CN)$_3$, Nat. Phys. **5**, 44 (2009).

[19] T. Itou, A. Oyamada, S. Maegawa, M. Tamura, and R. Kato, Quantum spin liquid in the spin-1/2 triangular antiferromagnet $EtMe_3Sb[Pd(dmit)_2]_2$, Phys. Rev. B **77**, 104413 (2008).

[20] M. Yamashita, N. Nakata, Y. Senshu, M. Nagata, H. M. Yamamoto, R. Kato, T. Shibauchi, and Y. Matsuda, Highly mobile gapless excitations in a two-dimensional candidate quantum spin liquid, Science **328**, 1246 (2010).

[21] S. Yamashita, T. Yamamoto, Y. Nakazawa, M. Tamura, and R. Kato, Gapless spin liquid of an organic triangular compound evidenced by thermodynamic measurements, Nat. Commun. **2**, 275 (2011).

[22] T. Yoshioka, A. Koga, and N. Kawakami, Quantum phase transitions in the Hubbard model on a triangular lattice, Phys. Rev. Lett. **103**, 036401 (2009).

[23] M. Laubach, R. Thomale, C. Platt, W. Hanke, and G. Li, Phase diagram of the Hubbard model on the anisotropic triangular lattice, Phys. Rev. B **91**, 245125 (2015).

[24] K. Misumi, T. Kaneko, and Y. Ohta, Mott transition and magnetism of the triangular-lattice Hubbard model with next-nearest-neighbor hopping, Phys. Rev. B **95**, 075124 (2017).

[25] T. Shirakawa, T. Tohyama, J. Kokalj, S. Sota, and S. Yunoki, Ground-state phase diagram of the triangular lattice Hubbard model by the density-matrix renormalization group method, Phys. Rev. B **96**, 205130 (2017).

[26] A. Szasz, J. Motruk, M. P. Zaletel, and J. E. Moore, Chiral spin liquid phase of the triangular lattice Hubbard model: A density matrix renormalization group study, Phys. Rev. X **10**, 021042 (2020).

[27] A. Szasz and J. Motruk, Phase diagram of the anisotropic triangular lattice Hubbard model, Phys. Rev. B **103**, 235132 (2021).

[28] B.-B. Chen, Z. Chen, S.-S. Gong, D. N. Sheng, W. Li, and A. Weichselbaum, Quantum spin liquid with emergent chiral order in the triangular-lattice Hubbard model, Phys. Rev. B **106**, 094420 (2022).

[29] S.-S. Lee and P. A. Lee, U(1) gauge theory of the Hubbard model: Spin liquid states and possible application to $\kappa-(BEDT-TTF)_2Cu_2(CN)_3$, Phys. Rev. Lett. **95**, 036403 (2005).

[30] T.-K. Ng and P. A. Lee, Power-law conductivity inside the Mott gap: Application to $\kappa-(BEDT-TTF)_2Cu_2(CN)_3$, Phys. Rev. Lett. **99**, 156402 (2007).

[31] T. Senthil, Theory of a continuous Mott transition in two dimensions, Phys. Rev. B **78**, 045109 (2008).

[32] D. Podolsky, A. Paramekanti, Y. B. Kim, and T. Senthil, Mott transition between a spin-liquid insulator and a metal in three dimensions, Phys. Rev. Lett. **102**, 186401 (2009).

[33] S. Banerjee, W. Zhu, and S.-Z. Lin, Electromagnetic signatures of chiral quantum spin liquid, npj Quantum Mater. **8**, 63 (2023).

[34] A. H. MacDonald, S. M. Girvin, and D. Yoshioka, $\frac{t}{U}$ expansion for the Hubbard model, Phys. Rev. B **37**, 9753 (1988).

[35] T. Cookmeyer, J. Motruk, and J. E. Moore, Four-spin terms and the origin of the chiral spin liquid in Mott insulators on the triangular lattice, Phys. Rev. Lett. **127**, 087201 (2021).

[36] L. Zhang and Z.-Y. Weng, Sign structure, electron fractionalization, and emergent gauge description of the Hubbard model, Phys. Rev. B **90**, 165120 (2014).

[37] D. N. Sheng, Y. C. Chen, and Z. Y. Weng, Phase string effect in a doped antiferromagnet, Phys. Rev. Lett. **77**, 5102 (1996).

[38] K. Wu, Z. Y. Weng, and J. Zaanen, Sign structure of the $t-J$ model, Phys. Rev. B **77**, 155102 (2008).

[39] K. Wu, Z.-Y. Weng, and J. Zaanen, Statistical fluxes and the Curie-Weiss metal state, Phys. Rev. B **84**, 113113 (2011).
[40] See Supplemental Material at http://link.aps.org/supplemental/10.1103/PhysRevB.109.L081116 for further details on analytical derivation and numerical calculation, which also includes Refs. [59,60].
[41] Z. Y. Weng, D. N. Sheng, Y.-C. Chen, and C. S. Ting, Phase string effect in the t-J model: General theory, Phys. Rev. B **55**, 3894 (1997).
[42] Z.-Y. Weng, Superconducting ground state of a doped Mott insulator, New J. Phys. **13**, 103039 (2011).
[43] Z. Zhu, D. N. Sheng, and A. Vishwanath, Doped Mott insulators in the triangular-lattice Hubbard model, Phys. Rev. B **105**, 205110 (2022).
[44] S. A. Chen, Q. Chen, and Z. Zhu, Proposal for asymmetric photoemission and tunneling spectroscopies in quantum simulators of the triangular-lattice Fermi-Hubbard model, Phys. Rev. B **106**, 085138 (2022).
[45] X.-Y. Song, A. Vishwanath, and Y.-H. Zhang, Doping the chiral spin liquid: Topological superconductor or chiral metal, Phys. Rev. B **103**, 165138 (2021).
[46] Y. Gannot, Y.-F. Jiang, and S. A. Kivelson, Hubbard ladders at small U revisited, Phys. Rev. B **102**, 115136 (2020).
[47] A. Wietek, J. Wang, J. Zang, J. Cano, A. Georges, and A. Millis, Tunable stripe order and weak superconductivity in the Moiré Hubbard model, Phys. Rev. Res. **4**, 043048 (2022).
[48] V. Zampronio and T. Macrì, Chiral superconductivity in the doped triangular-lattice Fermi-Hubbard model in two dimensions, Quantum **7**, 1061 (2023).
[49] Y. Zhang and L. Fu, Pseudogap metal and magnetization plateau from doping Moiré Mott insulator, SciPost Phys. Core **6**, 038 (2023).
[50] W. Kadow, L. Vanderstraeten, and M. Knap, Hole spectral function of a chiral spin liquid in the triangular lattice Hubbard model, Phys. Rev. B **106**, 094417 (2022).
[51] N. Gneist, L. Classen, and M. M. Scherer, Competing instabilities of the extended Hubbard model on the triangular lattice: Truncated-unity functional renormalization group and application to Moiré materials, Phys. Rev. B **106**, 125141 (2022).
[52] X. Lu, J.-X. Zhang, S.-S. Gong, D. N. Sheng, and Z.-Y. Weng, Sign structure in the square-lattice t-t'-J model and numerical consequences, arXiv:2303.13498.
[53] C. Peng, Y.-F. Jiang, Y. Wang, and H.-C. Jiang, Gapless spin liquid and pair density wave of the Hubbard model on three-leg triangular cylinders, New J. Phys. **23**, 123004 (2021).
[54] Y. Huang, S.-S. Gong, and D. N. Sheng, Quantum phase diagram and spontaneously emergent topological chiral superconductivity in doped triangular-lattice Mott insulators, Phys. Rev. Lett. **130**, 136003 (2023).
[55] Z. Zhu and Q. Chen, Superconductivity in doped triangular Mott insulators: The roles of parent spin backgrounds and charge kinetic energy, Phys. Rev. B **107**, L220502 (2023).
[56] F. Chen and D. N. Sheng, Singlet, triplet, and pair density wave superconductivity in the doped triangular-lattice moiré system, Phys. Rev. B **108**, L201110 (2023).
[57] H. Schlömer, U. Schollwöck, A. Bohrdt, and F. Grusdt, Kinetic-to-magnetic frustration crossover and linear confinement in the doped triangular $t-J$ model (2023), arXiv:2305.02342.
[58] H.-C. Jiang, Superconductivity in the doped quantum spin liquid on the triangular lattice, npj Quantum Mater. **6**, 71 (2021).
[59] W. Marshall and R. E. Peierls, Antiferromagnetism, Proc. R. Soc. London A **232**, 48 (1955).
[60] R.-Q. He and Z.-Y. Weng, On the possibility of many-body localization in a doped Mott insulator, Sci. Rep. **6**, 35208 (2016).